

Voltage Security Assessment and Control System using a Hybrid Intelligent Method

Worawat Nakawiro, *Student Member, IEEE*, and Istvan Erlich, *Senior Member, IEEE*

Abstract-- This paper presents a new hybrid intelligent algorithm for assessing and enhancing voltage security. The problem is decomposed into two stages. Firstly, the security of current operating point is assessed by learning vector quantization (LVQ) network according to the pre-specified criterion. Throughout the paper, continuation power flow (CPF) is adopted as a tool for defining voltage security margin (VSM). If an insecure state is indicated by the LVQ, the power system operator is given the suggestion for appropriate control settings so as to maintain the specified security level. In the second stage, the optimal reactive power dispatch (ORPD) problem is formulated and VSM is considered as an additional constraint. To include VSM determined by CPF along the optimization process, feed-forward neural network (FFNN) is trained to learn and perform similarly to CPF to relieve the intensive computing requirement. Ant colony optimization (ACO) is applied to handle the VSM constrained ORPD problem. The proposed method was tested on IEEE 30-bus system and successful results were obtained.

Index Terms-- Learning vector quantization; Artificial neural network; Ant colony optimization; Voltage security assessment and control

I. INTRODUCTION

IN recent years, voltage stability has been reported as one of the reasons of the blackouts all over the world in the last three decades [1]. This phenomenon occurs as a result of a contingency, such as loss of an important transmission line or a generator in combination with inadequate reactive power support at critical buses.

Even though the phenomenon is dynamic, it has been shown that under certain considerations a static approach is sufficient for the analysis. There have been several indicators proposed based on the static model to evaluate voltage security [2]. However, most of these indicators share the same weakness in that they are not expressed as a function of the system quantities reflecting physical meanings. On the other hand, PV curve determined by the continuation power flow (CPF) technique is among the most practical and widely-used technique to assess the voltage security of a power system [2]-[3]. The distance from the current operating point to the collapse point is defined as voltage security margin (VSM).

This method has been proven that it is capable of determining the voltage collapse point accurately and identifying critical buses. In addition to assessment of voltage security level, the system operators are interested to have information to apply proper control actions when the power system experiences or shows vulnerability to voltage stability.

Many researchers have demonstrated that voltage security margin can be enlarged by providing sufficient amount of reactive power at appropriate locations i.e.[4]-[5]. To achieve this task, optimal reactive power dispatch (ORPD) is formulated as a mixed-integer nonlinear optimization problem because transformer tap ratio and output of shunt capacitors/reactors have a discrete nature while generator bus voltage magnitudes have a continuous nature. The objective of ORPD is to minimize the total active power loss (P_{loss}) whereby VSM is treated as an additional constraint besides bus voltage limits, line flow limits, etc.

Several methods such as mathematical programming, fuzzy, or expert system have been developed for ORPD. However, these techniques may not be efficient in dealing with inequality constraints, nonlinearity of the objective function or discrete decision variables. Furthermore, some of these conventional methods often get stuck to local optimum. In recent years, a number of heuristic optimization methods have been extensively researched and applied to various problems in power systems [6].

Ant colony optimization (ACO) is the algorithm inspired by the foraging behavior of real ants and was initially proposed to solve combinatorial optimization problems [7]-[8]. It is only recently that there have been attempts to extend ACO to optimize a function in continuous domain. Among these methods, the method proposed by Socha and Dorigo in [9] called ACO_R , which reserves intrinsic concepts of ant algorithm, is shown to be more effective than other ant-related algorithms.

In this paper, we propose a two stage scheme for voltage security problem that consists of a security assessment at the first level and voltage security enhancement in the second level. Learning vector quantization (LVQ) capable of classifying the current operating condition whether it is voltage secure or insecure is developed. If the voltage insecure status is indicated by LVQ, ACO_R is deployed for ORPD with the aim to enhance voltage security. This paper is organized as follows. The proposed scheme is explained in section II. The approach of generating database for training neural networks is discussed in section III. The ACO_R and its modification for constraint optimization are explained in section IV. The optimal reactive power dispatch is formulated and the

W. Nakawiro and I. Erlich are with Institute of Electric Power Systems, University of Duisburg-Essen, Duisburg, 47057, Germany (e-mails: worawat.nakawiro@uni-due.de and istvan.erlich@uni-due.de)

implementation procedure is given in section V. In section VI, we present simulation results of the proposed scheme on the IEEE-30 bus system. Finally, summary discussion and future outlook are given in section VII.

II. THE PROPOSED SCHEME

The operating conditions of a power system are characterized by a number of variables. Therefore, an operating condition can be represented by an input vector of n dimension in pattern space R^n . This information can be obtained through the data acquisition installed as a part of SCADA system. Based on this set of data, the magnitude of output variable is employed to indicate the level of voltage security. In this paper, we use learning vector quantization [10] (LVQ) to classify the degree of voltage security margin of a power system into two classes namely “secure” and “insecure”. LVQ is trained offline with historical data saved in SCADA.

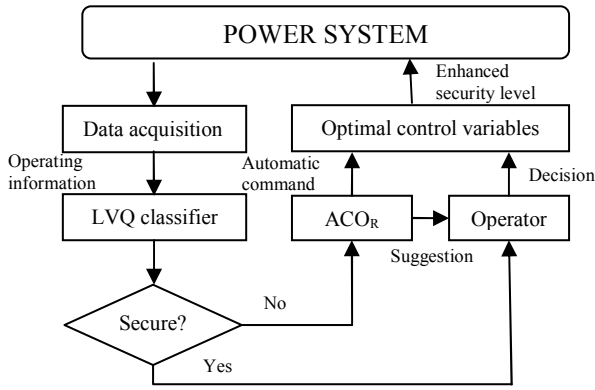


Fig. 1 The proposed scheme

For an insecure operating condition, the voltage security enhancement scheme which is formulated as optimal reactive power dispatch with a voltage security constraint is triggered. As mentioned earlier that there are a number of techniques used to detect the point of voltage collapse and insecurity. Among these, continuation power flow is proved to be efficient and of practical use.

However, solving CPF of an operating condition requires a number of power flow calculations along the load increase trajectory. It should be also noted that ACO_R is a population based technique and if it is applied to solve the ORPD problem, a large number of power flow analyses have to be called for to check feasibility of decision variables under investigation. Considering the ACO_R with the population of 20 as an example, if 150 generations are required for ACO_R to achieve the optimal solution, then power flow program has to be called in the optimization loop for 3000 (20×150) times. If CPF is incorporated to determine VSM along the optimization loop, then the CPF program has to be run for 3000 times in addition to the normal power flow program. Let us suppose further if a single CPF process requires 5 power flow solutions, then 15,000 different power flow solutions are required. This is quite a very cumbersome task and thereby would add a high degree of complexity to the overall

algorithm. Due to this reason, VSM evaluation is carried out independently from the optimization loop in literature [11]-[12]. Voltage security level is checked by running CPF only at the final generation. The best individual of that set is first selected and its corresponding variables are used to set up CPF analysis to check if the feasibility of VSM.

In this paper, we attempt to use a feed-forward neural network [13] well trained offline to perform the task of CPF during ACO_R optimization.

III. DATABASE GENERATION

Database for training and testing ANNs is generated to simulate different operating conditions including random load distribution, random generation distribution and line outages that the test system would experience in a day. The daily load profile and forecasting error reflecting some uncertainties are assumed as shown in Fig. 1.

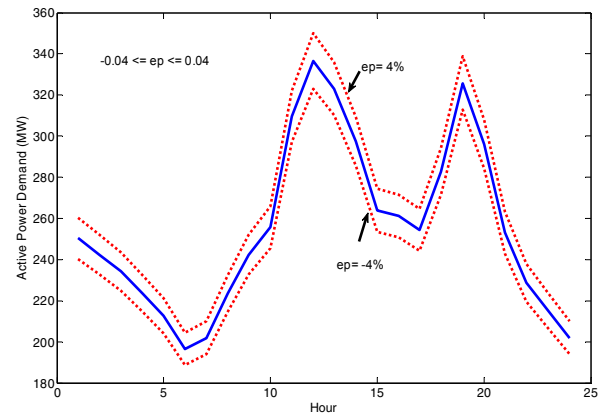


Fig. 2 Daily load curve for database generation

The total real and reactive power demand of pattern i can be found from, respectively;

$$P_{Ci} = P_{BC}^t(1 + ep) \quad (1)$$

$$Q_{Ci} = Q_{BC}^t(1 + ep) \quad (2)$$

where P_{BC} and Q_{BC} are base case real and reactive power taken from the daily load curve at hour t ; ep is the load forecast error ($\pm 4\%$ is assumed). P_{Ci} and Q_{Ci} are shared among load buses based on a vector of normalized uniform random distribution defined by

$$\mathbf{k} = [k_1 \ k_2 \ \dots \ k_n]^T \quad (3)$$

where $\sum_{i=1}^{N_{PQ}} k_i = 1$ and N_{PQ} is the number of load buses. The generated active power of the slack bus changes according to

$$P_{Gs} = x_{pg} P_G; \quad 0.2 \leq x_{pg} \leq 0.6 \quad (4)$$

The rest of generation requirement which is $(1 - x_{pg})P_G$ MW is randomly distributed to the other generators according to

$$P_{Gi} = (1 - x_{pg})P_G k_{mi}; \quad \forall i [i \in \mathbf{PV} \wedge i \notin \mathbf{G}_s] \quad (5)$$

$$\mathbf{km} = [k_{m1} \ k_{m2} \ \dots \ k_{mp}]^T \quad (6)$$

where P_{Gi} is the real power generation of generator i , \mathbf{km} the vector of normalized random distribution factor; \mathbf{PV} is the

set of generators; \mathbf{G}_s is the set of slack generators; p is the number of generators excluding the slack.

IV. ANT COLONY OPTIMIZATION

As mentioned earlier, one of the most recent ant-based optimization methods is the ACO_R algorithm. In this section, the original ACO_R is modified to suit the requirement for mixed integer nonlinear optimization problem and capable of handling equality and inequality constraints.

In contrast to discrete ant algorithms where pheromone information is stored in a table form and sampling is done based on a discrete probability distribution function (PDF), ACO_R uses a Gaussian kernel PDF to model multi-promising area of the search space. An example of a Gaussian kernel PDF defined by (7) is shown in Fig.3:

$$G^i(x) = \sum_{l=1}^k \omega_l g_l^i(x) = \sum_{l=1}^k \omega_l \frac{1}{\sigma_l^i \sqrt{2\pi}} e^{-\frac{(x-\mu_l^i)^2}{2(\sigma_l^i)^2}} \quad (7)$$

where k is the number of single Gaussian PDF at i construction step; ω , μ , and σ are vectors of size k defining the weights, means and standard deviations associated with every individual Gaussian PDF at the i construction step.

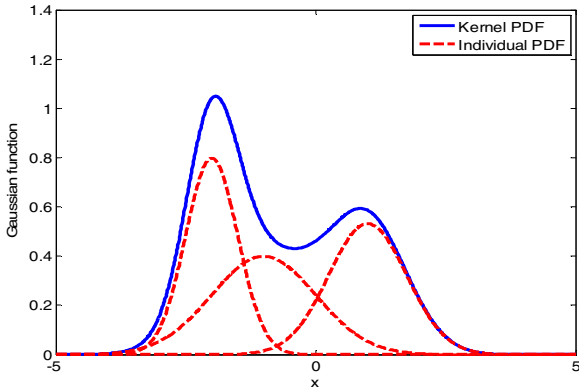


Fig. 3 An example of Gaussian kernel PDF ($\omega_l=1$ for all three individual PDFs is assumed)

When applying Gaussian kernel PDF for sampling, it is a general approach that the inverse of cumulative distribution function (CDF), $D^{-1}(x)$, is used. However, it is not always straightforward to find D^{-1} of an arbitrary PDF. Therefore, an alternative sampling technique is used in this paper in order to increase flexibility of the implementation. This can be done in two phases. First, the weight ω_l of the l solution is computed from:

$$\omega_l = \frac{1}{qk\sqrt{2\pi}} e^{-\frac{(l-1)^2}{2q^2k^2}} \quad (8)$$

where q is a parameter of the algorithm and k is the size of archive. When q is small, the best rank solutions in the archive have very strong influences in guiding new search directions where a larger q allows the wider search diversification. In the first step, one of Gaussian PDFs constituting the Gaussian kernel is chosen based on probability defined by;

$$p_l = \frac{\omega_l}{\sum_{r=1}^k \omega_r}; \forall l=1,2,\dots,k \quad (9)$$

Then, for each ant the Roulette wheel selection method is applied to randomly select the solution rank l for calculating mean and standard deviation in the next step.

The ACO_R stores a pre-specified number of solutions in a set called a solution archive T . Fig. 4 shows the structure of the solution archive designed to handle constrained optimization problems. The last column of T indicates feasibility of the solution in terms of constraint violation. The solutions in T are used to generate the ant population based on the triplet parameters ω , μ , and σ in sequential construction steps.

Once the rank of l is selected, the vector of mean μ_i is defined as:

$$\mu_l^i = s_l^i; \forall i=1,2,\dots,n \quad (10)$$

where n is the problem dimension and k is the number of archive solutions. Standard deviation σ for every construction step i is calculated from the average distance from the chosen solution s_l to the other solutions saved in T and multiplied by the factor ξ . The parameter ξ has the same characteristic as the coefficient of pheromone evaporation in a conventional ACO. Based on determined mean and standard deviation, a corresponding random variable can be generated by a technique, such as Box and Mueller [14].

After a complete generation, all solutions in T are ranked according to their feasibility status and fitness value. Because the archive solutions with lower ranks have the greater influence in guiding the search directions, feasible solutions are first ranked based on their fitness values found by the self-adaptive penalty scheme in [15]. The same process is repeated for infeasible solutions, which are placed in the lower portion of T .

s_1	s_1^1	s_1^2	\dots	s_1^j	\dots	s_1^n	$f(s_1)$	p_1	1
s_2	s_2^1	s_2^2	\dots	s_2^j	\dots	s_2^n	$f(s_2)$	p_2	1
\vdots	\vdots	\vdots	\vdots	\vdots	\vdots	\vdots	\vdots	\vdots	\vdots
s_l	s_l^1	s_l^2	\dots	s_l^j	\dots	s_l^n	$f(s_l)$	p_l	0
\vdots	\vdots	\vdots	\vdots	\vdots	\vdots	\vdots	\vdots	\vdots	\vdots
s_k	s_k^1	s_k^2	\dots	s_k^j	\dots	s_k^n	$f(s_k)$	p_k	0
	G^1	G^2	G^j	G^n					

Fig. 4 Data structure of the archive solution

For constrained optimization problems, the attraction of a solution s_l is measured by the value of fitness function instead of the value of objective function. Therefore, the objective function of ACO_R is modified to the sum of the distance value, $d(\mathbf{x})$ and the penalty value, $p(\mathbf{x})$.

$$\text{Minimize } f^*(\mathbf{x}) = d(\mathbf{x}) + p(\mathbf{x}) \quad (11)$$

The distance function is defined as follows:

$$d(\mathbf{x}) = \begin{cases} v'(\mathbf{x}) & \text{if } r_f = 0 \\ \sqrt{f'(\mathbf{x})^2 + v'(\mathbf{x})^2} & \text{otherwise} \end{cases} \quad (12)$$

where r_f is the ratio of the number of feasible solutions in the archive or ant population. $f'(\mathbf{x})$ is the normalized value of $f(\mathbf{x})$ and $v'(\mathbf{x})$ is the sum of normalized violation of each constraint divided by the number of constraints. When there is no feasible solution in the population, the objective function is now to minimize the constraint violation. If there are feasible solutions, then the distance value becomes the root mean square of the sum of the objective value and constraint violations. This process can help improve the search performance of ACO_R because it guides the ants to concentrate only on the distance to feasible space when there is a drought of feasible solutions. When a number of feasible solutions have been explored, the ants still continues to search for further feasible region and simultaneously trace the optimal area.

The second term of (11) is called the penalty value. This term is very helpful at a given generation of ACO_R to identify which ant can help the exploration. The idea of this term is to ensure that the most useful ant both in terms of infeasible solutions (at the early stage) and feasible solutions (toward the end) are assigned lower penalties relative to other ant solutions. Therefore $p(\mathbf{x})$ can be defined as shown below:

$$p(\mathbf{x}) = (1 - r_f)X(\mathbf{x}) + r_f Y(\mathbf{x}) \quad (13)$$

where

$$X(\mathbf{x}) = \begin{cases} 0 & \text{if } r_f = 0 \\ v'(\mathbf{x}) & \text{otherwise} \end{cases} \quad (14)$$

$$Y(\mathbf{x}) = \begin{cases} 0 & \text{if } \mathbf{x} \text{ is infeasible} \\ b'(\mathbf{x}) & \text{if } \mathbf{x} \text{ is feasible} \end{cases} \quad (15)$$

The discrete variables such as positions of transformer tap changers and settings of shunt compensators are normalized and converted to integers $(0, 1, \dots, n)$, where n corresponds the number of position settings. Initially, integer variables are randomly generated within their boundaries. Later when ant solutions are randomly sampled from the archive, the corresponding value is rounded off to its nearest integer.

V. OPTIMAL REACTIVE POWER DISPATCH

The solution of the optimal reactive power dispatch involves the optimization of the summation of active power loss on individual lines subject to various nonlinear constraints. This optimization task can be carried out in two stages: planning and operation. In the planning stage, system behaviors of different scenarios can be calculated. During the operation, an optimization algorithm is used to suggest the efficient operation scheme as per grid requirements.

A. Problem Formulation

The problem described above can be mathematically expressed as follows:

$$\text{Minimize} \quad f(\mathbf{x}) = P_{loss}(\mathbf{x}, \mathbf{d}) \quad (16)$$

subject to

a) Generator bus voltage limits

$$u_{Gi}^{\min} \leq u_{Gi} \leq u_{Gi}^{\max} \quad \forall i \in \mathbf{PV} \quad (17)$$

b) Shunt compensator limits

$$q_{Ci}^{\min} \leq q_{Ci} \leq q_{Ci}^{\max} \quad \forall i \in \mathbf{QC} \quad (18)$$

c) Transformer tap setting limits

$$a_i^{\min} \leq a_i \leq a_i^{\max} \quad \forall i \in \mathbf{T} \quad (19)$$

d) Load bus voltage limits

$$u_{Li}^{\min} \leq u_{Li} \leq u_{Li}^{\max} \quad \forall i \in \mathbf{PQ} \quad (20)$$

e) Line flow limits

$$s_{Li}^{\min} \leq s_{Li} \leq s_{Li}^{\max} \quad \forall i \in \mathbf{L} \quad (21)$$

f) Voltage security margin limit

$$VSM \geq VSM^{\text{limit}} \quad (22)$$

where P_{loss} is the total active power loss in the transmission system; \mathbf{PV} is the set of generator (PV) buses; \mathbf{QC} is the set of shunt compensators; \mathbf{T} is the set of transformers; \mathbf{PQ} is the set of load (PQ) buses; \mathbf{L} is the set of transmission lines. The vector \mathbf{x} contains control variables listed in (17)-(19) where (17) is treated as continuous variables and (18) to (19) are treated as discrete variables. The vector \mathbf{d} describes the condition of active and reactive power demand and active power generation. Based on appropriate selected inputs, VSM in (22) is determined from the FFNN properly trained in the offline mode.

The implementation steps of the proposed methodology can be written as follows;

- Step 1: Prepare the training and testing data sets.
- Step 2: In offline mode, carry out the LVQ (as classifier) and FFNN (as CPF replacement) trainings and evaluate the training performance. If succeeded, go to step 3; otherwise resume with larger data sets or change parameters.
- Step 3: Apply testing data set to the developed LVQ.
- Step 4: Classify operating conditions as "secure" or "insecure".
- Step 5: For "insecure" operating conditions, starts the ORPD module as formulated in (16)-(22).
- Step 6: Start ACO_R procedures

The details of ACO_R algorithm can be summarized as.

- Step 6.1: Randomly initialize the archive solution of ACO_R within respective limits.
- Step 6.2: For each individual in the archive, run power flow program to find the corresponding operating condition. Use the trained FFNN to determine (22).
- Step 6.3: Evaluate the fitness of each individual based on the strategy described in (11) to (15);
- Step 6.4: Rank individuals of the archive based on feasibility and fitness values.
- Step 6.5: Perform random sampling based on Gaussian kernel PDF as described in section IV to generate the ant population and evaluate fitness values.
- Step 6.6: Find the generation best ($pbest$) and global best ($gbest$) ant based on the following criteria;
 - a) Any feasible solution is preferred to any infeasible solution;
 - b) Among two feasible solutions, the one having better objective value is preferred;

- c) Among two infeasible solutions, the one having smaller fitness value (smaller constraint violation) is preferred.

- Step 6.7: Store $pbest$ and $gbest$
- Step 6.8: Update the archive solutions by replacing a pre-specified number of worse solutions by the same amount of better ant solutions and reevaluate the fitness of archive solutions.
- Step 6.9: Repeat steps 6.5 to 6.8 until the stopping criterion is satisfied.
- Step 7: Repeat step 6, for other insecure operating conditions.
- Step 8: Evaluate the performance of the overall algorithm.

VI. SIMULATION RESULTS

The IEEE 30-bus system is used to test the effectiveness of the proposed algorithm. The test system used in this study has six generation buses located at buses 1,2,5,8,11 and 13, 24 load buses, 4 on-load tap changing (OLTC) transformers and 41 transmission lines. The reactive power (Q) sources are connected to buses 10 13 15 16 18 20 25 27 and 30. All OLTCs and Q sources are considered as discrete variables with 21 steps. Therefore, the dimension of the vector of control variables is 20. The test system, parameters and initial bus data are discussed in detail in [16]. The limits of control variables are given in Appendix.

The software package namely, UWPflow [17]-[18], is utilized to prepare the training and testing patterns for LVQ and FFNN. Fig.5 shows PV curves of two different operating states. The load parameter λ corresponding to the nose point of the PV curve represents VSM of the power system at that particular operating condition.

In this paper, the voltage security level is classified into two levels namely secure and insecure according to the value of λ : secure ($\lambda > 0.25$) and insecure ($\lambda \leq 0.25$). The ranges of voltage security level that are dependent on the studied power system under various operating conditions are statistically determined. The neural network toolbox of MATLAB was utilized for LVQ and FFNN. The ACO_R algorithm was also developed in MALAB.

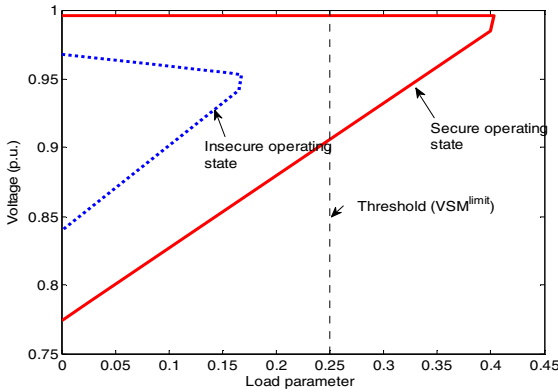


Fig. 5 VSM of different operating conditions

Due to the limitation of neural networks in learning functional relationship between system operating information and the predicted output when the system topology changes, a distinct neural network is usually required for each network

topology [19]. In this paper, we present extensive simulation results of one of the critical contingency conditions. The identical procedures can be also applied to solve the other cases.

Before the developed neural networks (both LVQ and FFNN) can be applied, the performance of both networks has to be verified according to the following criteria.

For LVQ, the performance of classification can be justified by three indicators namely success rate, false alarm rate and missed alarm rate. The success rate is defined as the ratio of the number of correctly classified patterns to the total number of patterns. The false alarm rate is the ratio of the number of secure operating conditions (OCs) that are classified as insecure OCs while the missed alarm rate is the ratio of the number of insecure operating conditions (OCs) that are classified as secure OCs.

For FFNN, the performance of regression can be evaluated by the maximum error (e_{max}) and RMS error (e_{rms}) defined as follows:

$$e_{max} = \max \{ |T_q - O_q| \}, q = 1, 2, \dots, NO \quad (23)$$

$$e_{rms} = \sqrt{\frac{1}{p^{max}} \sum_{p=1}^{p^{max}} \frac{1}{NO} \sum_{q=1}^{NO} [t_{qp} - o_{qp}]^2} \quad (24)$$

where $T_q = [t_{q1}, t_{q2}, \dots, t_{qp}^{max}]^T$ is the target vector of q^{th} neuron of the output layer; $O_q = [o_{q1}, o_{q2}, \dots, o_{qp}^{max}]^T$ is the output vector of q^{th} neuron of the output layer; p^{max} is the maximum number of patterns and NO is the number of neuron of the output layer.

Under the contingency condition, a single line outage (line 21-1) is simulated. 5,000 different operating points were generated according to the method presented in section III for training and testing FFNN. Since we intend to apply this FFNN to approximate VSM in the ORPD problem, therefore the control variables listed in (17) to (19) must be randomly varied within their respective boundaries.

A three-layer FFNN with 20 hidden layer neurons is trained with Bayesian regularization in order to improve the generalization property. Even a number of changes in load demand and control parameters were considered, the developed FFNN is reasonably efficient to map the underlying input-output relationship with $e_{max} = 0.3168$ and $e_{rms} = 0.0397$.

In this paper, the input vector describing a power system state is described by;

$$X_i = [sL_{i1}, sL_{i2}, \dots, sL_{im}, u_{i1}, u_{i2}, \dots, u_{in}, O_i]^T \quad (25)$$

where sL_{ik} is the MVA power flow over line k for state i ; u_{ij} is the control variable j for state i ; O_i is target value of state i ; m is the number of selected transmission line ($m=10$); n is the number of control variables associated in ORPD ($m=19$). The dimension and statistical characteristic of an input vector plays a very important role in learning of a neural network. Principal component analysis (PCA) [13] is therefore applied to eliminate redundant input information so that the number of input features is reduced and the learning performance is

increased.

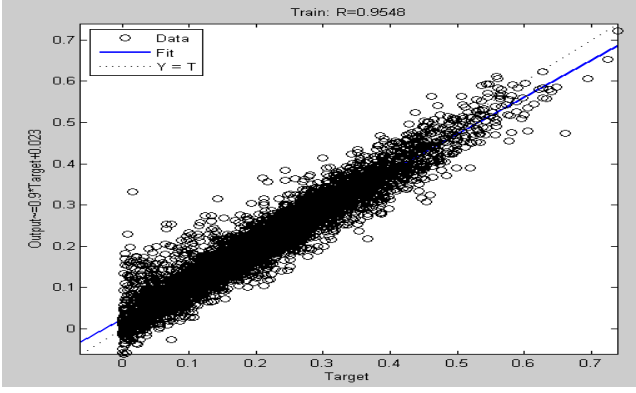


Fig.6 Post regression of training dataset

The developed FFNN is now tested with 150 unforeseen input patterns to verify the performance. Fig.7 shows the percentage of estimation error determined by the difference between the actual and estimated VSM . It can be observed that the estimation error of FFNN is reasonably acceptable.

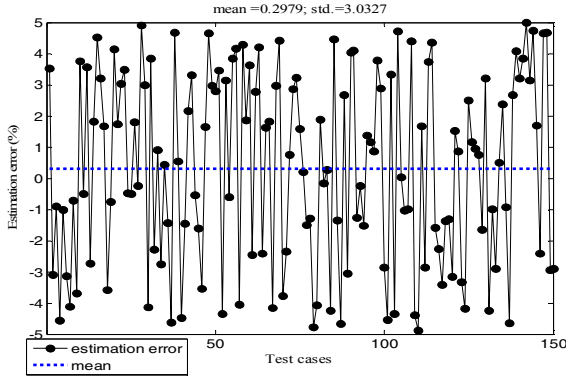


Fig.7 Estimation error of testing dataset

Based on the same input vector shown in (25), LVQ as a voltage security classifier is trained by the data whose details are listed in Table I. Performance of LVQ classifier of 1000 unforeseen testing samples is shown in Table II. In this study, we find that the effectiveness of the developed LVQ is moderate. One of potential reasons of such non-superior performance of LVQ could be that we have assumed too many parameter changes in the phase of generating the knowledge base data. This could introduce a very high degree of complexity to the learning ability of LVQ. Further investigations are required on this aspect.

TABLE I. TWO-CLASS PARTITION FOR LVQ

Database	Training set	Testing set
5000	4000	1000
<u>Two-class partition by LVQ</u>		
Class A (secure)	1623	390
Class B (insecure)	2377	610

TABLE II. PERFORMANCE EVALUATION OF TWO-CLASS CLASSIFICATION

Classification of test set by LVQ		
For TS=4000	Class A	Class B
Samples of class A (390)	349	41
Samples of class B (610)	156	454
Classification performance evaluation		
Success rate	80.3%	(803/1000)
False alarm	10.51%	(41/390)
Missed alarm	25.57%	(156/610)

TS = size of training set

Ten operating conditions which were correctly classified by LVQ as voltage insecure are now considered for the voltage security enhancement scheme. Fig.8 shows the active power loss (P_{loss}) before and after the ACO_R optimization process of ten different operating states whereby Fig.9 depicts the corresponding voltage security margin (VSM). The parameters of ACO_R used in this paper are given in Table III.

TABLE III. ACO_R PARAMETER SETTINGS

Parameter	Value
Archive size (k)	40
Number of ants (n_{ant})	30
Convergence rate factor (q)	0.2
Pheromone evaporation (ξ)	0.99

It can obviously be observed that with optimal setting of control parameters P_{loss} of all operating conditions are significantly reduced. At the same time, all VSMs which were previously below the threshold limit ($VSM^{limit} = 0.25$) and classified as insecure states are now enhanced because VSM of all states are now greater than 0.25.

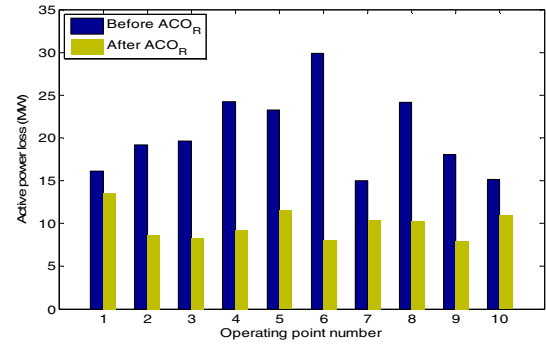


Fig.8 Comparison of active power loss before and after ACO_R

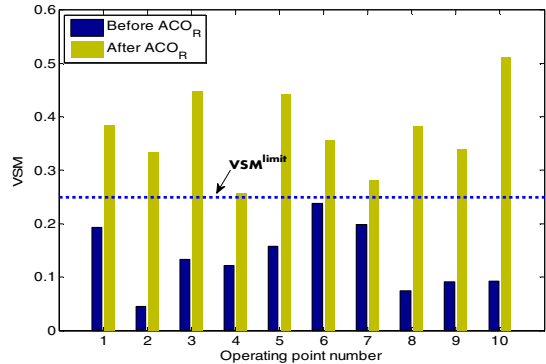


Fig.9 Comparison of voltage security margin before and after ACO_R

The active power loss of current best (p_{best}) and best-so (g_{best}) far solutions are plotted against the generation number in Fig.10 to demonstrate the performance of ACO_R . In this study based on experiments, the ACO_R stops if after 150 iteration there is no further improvement of g_{best} . Otherwise, the ACO_R continues until the maximum number of generation ($G_{max} = 200$) is reached. The variations of discrete control variables, settings of reactive power sources (at some selected locations) and transformer taps, are shown in Figs. 11-12, respectively. The variation of selected generator bus voltages which are continuous variables is shown in Fig. 13. In this three figures, it can be found that the the control variable changes are nearly constant within the maximum number of generations.

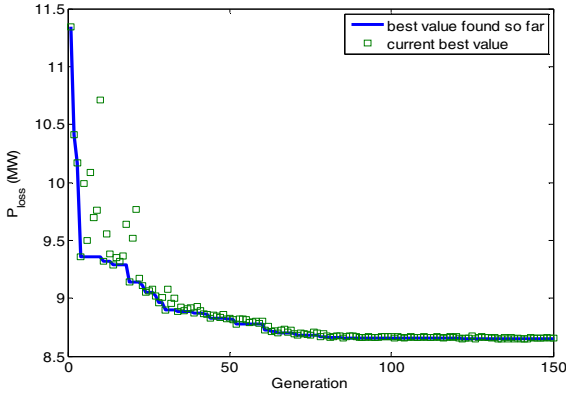


Fig.10 Variation of active power loss during ACO_R iterations

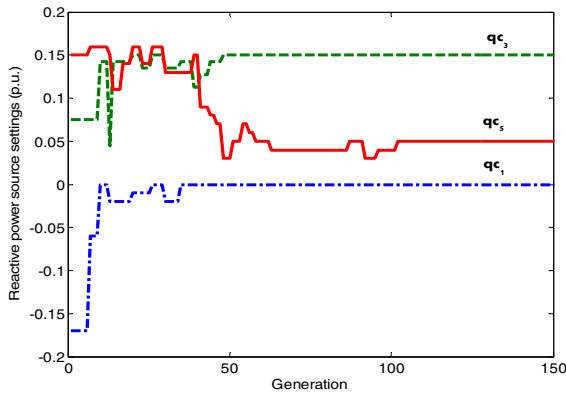


Fig.11 Variation of reactive power source settings during ACO_R iterations

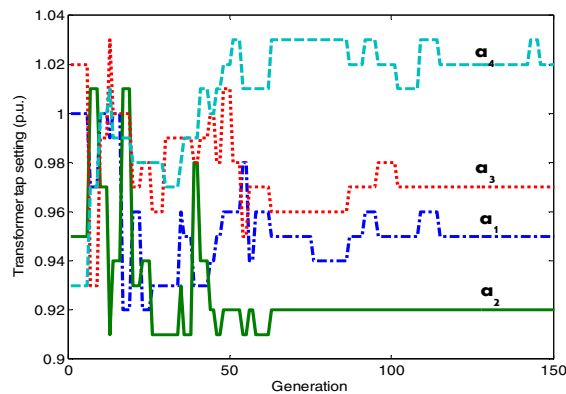


Fig.12 Variation of transformer tap settings during ACO_R iterations

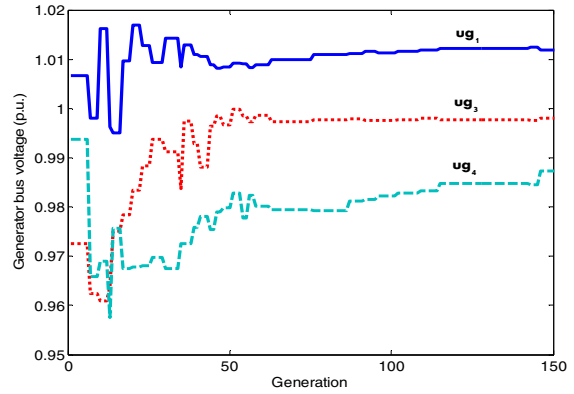


Fig.13 Variation of generator bus voltages during ACO_R iterations

VII. CONCLUSION

This paper investigates a two-stage design of online voltage security assessment and control tool. It is well accepted that deterministic computation methods produce the most accurate results. However, these approaches are computationally intensive and modeling simplifications are normally assumed in many cases. To overcome these limitations, intelligent system modules are currently implemented as a complementary part in addition to conventional simulation tools. The proposed method of this paper can utilize the historical information and knowledge from previous simulations to rapidly determine voltage security of a power system and at the same time suggesting the appropriate control settings if the voltage security enhancement is required.

A LVQ is applied in the first stage to classify if the current operating condition secure or insecure. In the second part, the optimal settings of control parameters to enhance the system security are either delivered to the system operator as a suggestion or automatically sent to the appropriate devices. Since CPF is a time-consuming process and its inclusion in the ORPD could be extremely cumbersome, a FFNN is trained to perform the task of CPF in determining VSM along the ACO_R process. MVA flows on the selected lines and settings of control parameters are chosen as the inputs of both LVQ and FFNN. Training neural networks for large power system with a number of changes in system parameters is quite a demanding task. Special cares have to be spent on many aspects, for example acquiring adequate number of sample data, selecting appropriate neural network architectures, etc. There are still challenges in designing an efficient single neural network to predict voltage security level of a power system of different contingencies and versatile operating scenarios.

The simulation results of ACO_R show the robustness of the algorithm in terms of providing solutions of a mixed-integer nonlinear programming problem. By appropriately adjusting control variables related to reactive power, active power loss is significantly minimized and thereby improving the security margin of the power system. The method presented in this paper could provide some idea in applying different computational intelligence systems to power system operations.

APPENDIX

TABLE IV. LIMITS OF GENERATOR BUS VOLTAGES AND TRANSFORMER TAP SETTINGS

Generator bus voltage limits (p.u.)				Transformer tap setting limits (p.u.)	
Slack generator		Other generators		a_i^{\min}	a_i^{\max}
u_{Gi}^{\min}	u_{Gi}^{\max}	u_{Gi}^{\min}	u_{Gi}^{\max}		
0.95	1.05	0.9	1.1	0.9	1.1

TABLE V. LIMITS OF REACTIVE POWER SOURCES

Bus no.	Reactive power source limits (p.u.)								
	10	13	15	16	18	20	25	27	30
q_{ci}^{\min}	-0.1	0	0	0	0	0	0	0	0
q_{ci}^{\max}	0	0.2	0.15	0.1	0.2	0.1	0.3	0.25	0.2

REFERENCES

- [1] T. Van Cutsem and C. Vournas, *Voltage stability of electric power systems*, Kluwer Academic Publisher, 1998
- [2] Voltage stability assessment: concepts, practises and tools, Aug. 2002, www.power.uwaterloo.ca [online]
- [3] V. Ajjarapu, *Computational techniques for voltage stability assessment and control*, Springer-Verlag, 2006
- [4] T. Van Cutsem, "A method to compute reactive power margin with respect to voltage collapse," *IEEE Trans. on Power Systems*, vol.6, no.1, pp.145-156, 1991
- [5] C.W. Liu, C.S. Chuang, and J.A. Jiang, "Genetic algorithms as a reactive power source dispatching aid for voltage security enhancement," In proc. Natl. Sci. Coun. ROC(A), vol. 25, no.1, 2001, pp. 53-62
- [6] K.Y. Lee and M.A. El-Sharkawi, *Modern heuristic optimization techniques: theory and applications to power systems*, Wiley-IEEE press, 2008
- [7] M. Dorigo, and L.M. Gambardella, "Ant colony system : a cooperative learning approach to the travelling salesman problem," *IEEE Trans. on Evolutionary Computation*, 1997, pp. 53-66
- [8] M. Dorigo and T. Stützle, *Ant colony optimization*, MIT press, Cambridge, MA, 2004
- [9] K. Socha and M. Dorigo, "Ant colony optimization for continuous domains," *European Journal of Operational Research*, vol.185, 2008, pp. 1155-1173
- [10] T. Kohonen, *Self-organizing maps*, Springer-Verlag, 1995
- [11] H. Yoshida, K. Kawata, Y. Fukuyama, S. Takayama and Y. Nakanishi, "A particle swarm optimization for reactive power and voltage control considering voltage security assessment", *IEEE Trans. on Power Systems*, vol. 15, no.4, Nov. 2000
- [12] M. Varadarajan and K.S. Swarup, "Network loss minimization with voltage security using differential evolution", *Elec. Power Syst. Res.*, vol.78, 2008, pp. 815-823
- [13] S. Haykin, *Neural networks: a comprehensive foundation*, Macmillian College Publishing, Canada, 1994
- [14] G.E.P. Box and M.E. Müller, "A note on the generation of reandom normal deviates," *Annals of mathematical statistics*, vol. 29, no.2, pp.610-611, 1958
- [15] B. Tessema, G.G. Yen, "A self adaptive penalty function based algorithm for constrained optimization," in proc. *IEEE Congress on Evolutionary Computation*, 2006, 16-21 July 2006, pp. 246-253
- [16] H. Saadat, *Power system analysis*, McGraw-Hill, 1999
- [17] C.A. Canizares, C.Z. DeSouza, and V.H. Quintana, "Comparison of performance indices for detection of voltage collapse," *IEEE Trans. on Power Systems*, vol.11, no.3, pp.1441-1450, 1994

- [18] C.A. Canizares and F.L. Alvarado, "Point of collapse and continuation method for AC/DC systems," *IEEE Trans. on Power Systems*, vol. 8, no.1, February 1003, pp.1-8
- [19] S. Chakrabarti and B. Jeyasurya, "Multicontingency voltage stability monitoring of a power system using an adaptive radial basis function network," *Elec. Power and Ener. Sys.*, vol.30, pp. 1-7, 2008

BIOGRAPHIES

Worawat Nakawiro received his B.Eng. degree in electrical engineering from Faculty of Engineering, Thammasat University, Thailand in 2002 and M.Eng. in electric power system management from Asian Institute of Technology, Thailand in 2004. He is currently a Ph.D. student at the University of Duisburg-Essen, Germany with financial support from DAAD. His research interests include computational intelligence with emphasis on heuristic optimization and its applications in power systems and voltage stability problems.

Istvan Erlich received his Dipl.-Ing. degree in electrical engineering from the Technical University of Dresden, Germany in 1976. After his study, he worked in Hungary in the field of electrical distribution networks. From 1979 to 1991, he joined the department of electrical power systems of the Technical University of Dresden again, where he received his PhD degree in 1983. In the period of 1991 to 1998, he worked with the consulting company EAB in Berlin and the Fraunhofer institute IITB Dresden, respectively. During this time, he also had teaching assignments at the Technical University of Dresden. Since 1998, he is a professor and head of the institute of electric power systems at the University of Duisburg-Essen, Germany. His major scientific interest is focused on power system stability and control, modeling and simulation of power system dynamics including intelligent system applications. He is a member of VDE and senior member of IEEE.